LATTICE DYNAMICS. PHASE TRANSITIONS

Lattice dynamics of a Rb_2KScF_6 crystal in unstable cubic and tetragonal phases and in a stable monoclinic phase

V. I. Zinenko*) and N. G. Zamkova

L. V. Kirenskiĭ Institute of Physics, Siberian Branch of the Russian Academy of Sciences, 660036 Krasnoyarsk, Russia

(Submitted December 8, 1998)
Fiz. Tverd. Tela (St. Petersburg) **41**, 1297–1305 (July 1999)

The results of a nonempirical calculation of the static and dynamic properties of a Rb_2KScF_6 crystal with elpasolite structure in cubic, tetragonal, and monoclinic phases are presented. The calculation is performed on the basis of a microscopic model of an ionic crystal that takes account of the deformability and polarizability of the ions. The deformability parameters of the ions are determined from the condition that the total energy of the crystal is minimum. The computational results for the equilibrium lattice parameters are in satisfactory agreement with experimental data. Unstable vibrational modes are found in the vibrational spectrum of the lattice in the cubic and tetragonal phases. These modes occupy the phase space throughout the entire Brillouin zone. The characteristic vectors of the most unstable mode at the center of the Brillouin zone of the cubic phase are related to the displacements of the fluorine ions and correspond to rotation of ScF_6 octahedra. Condensation of this mode leads to a tetragonal distortion of the structure. In the tetragonal phase the most unstable mode belongs to the boundary point of the Brillouin zone and condensation of this mode leads to monoclinic distortion with doubling of the unit-cell volume. In the monoclinic phase unstable modes are absent in the vibrational spectrum of the lattice.
[S1063-7834(99)03607-2]

Halides $A_2BB^{3+}X_6$ having the elpasolite structure undergo very diverse structural phase transitions associated with the lattice instability of the high-symmetry cubic phase. Uniform nonpolar distortions of the crystal lattice and distortions accompanied by a change in the unit-cell volume of the crystal are observed in the low-temperature phases in these compounds. Structural distortions in most crystals in this family are associated either with the locations of $B^{3+}X_6$ octahedra or a combination of rotations of octahedra and displacements of the A ions.

The instability of a crystal lattice with respect to normal vibrations, corresponding to rotations of octahedra, is apparently a characteristic feature of perovskite-like compounds. In most halides, and in some oxide crystals with perovskite structure, such an instability leads to structural phase transitions in low-symmetry phases with an increase in the unit-cell volume as compared to the volume of the initial cubic phase. The problem of structural instability of perovskite with respect to the ferroelectric lattice vibrational mode and with respect to the vibrational mode associated with rotations of octahedra has been under discussion in experimental and theoretical investigations for several decades now. In the last few years there have appeared many works wherein the phonon frequencies are calculated in one or another approach on the basis of first-principles density functional method for many members of the perovskite family and attempts have been made to understand the nature of this instability.

Virtually no calculations of the phonon spectrum of the crystal have been performed for crystals with elpasolite structure. At the same time these crystals are being intensively investigated by various experimental methods, and there now exist data on the structures of the low-symmetry phases, the physical properties, and the changes in the lattice at phase transitions, for many crystals in this family (see, for example, the recent review in Ref. 1).

Rb_2KScF_6 belongs to the elpasolite family and its crystal structure in the high-symmetry phase is cubic with space group $Fm3m$ and one molecule per unit cell (Fig. 1). As the temperature decreases, Rb_2KScF_6 undergoes two successive structural phase transitions: at $T_{c1}=250$ K to the tetragonal phase with space group $I4/m$ with no change of the cell volume as compared to the volume of the cubic phase and into the monoclinic phase at $T_{c2}=220$ K with space group $P12_1/n1$ and two molecules per unit cell. Structural investigations of low-symmetry phases[2] show that the distortions of the cubic structure in the tetragonal phase are mainly due to rotations of ScF_6 octahedra; these rotations are uniform throughout the entire volume of the crystal. Distortions in the low-temperature monoclinic phase are related to nonuniform rotations of ScF_6 octahedra and to displacements of rubidium ions from positions of equilibrium in the tetragonal phase.

Our objectives in the present work are to calculate, from first principles, the equilibrium volume, the total spectrum of lattice vibrations, and the high-frequency permittivity in

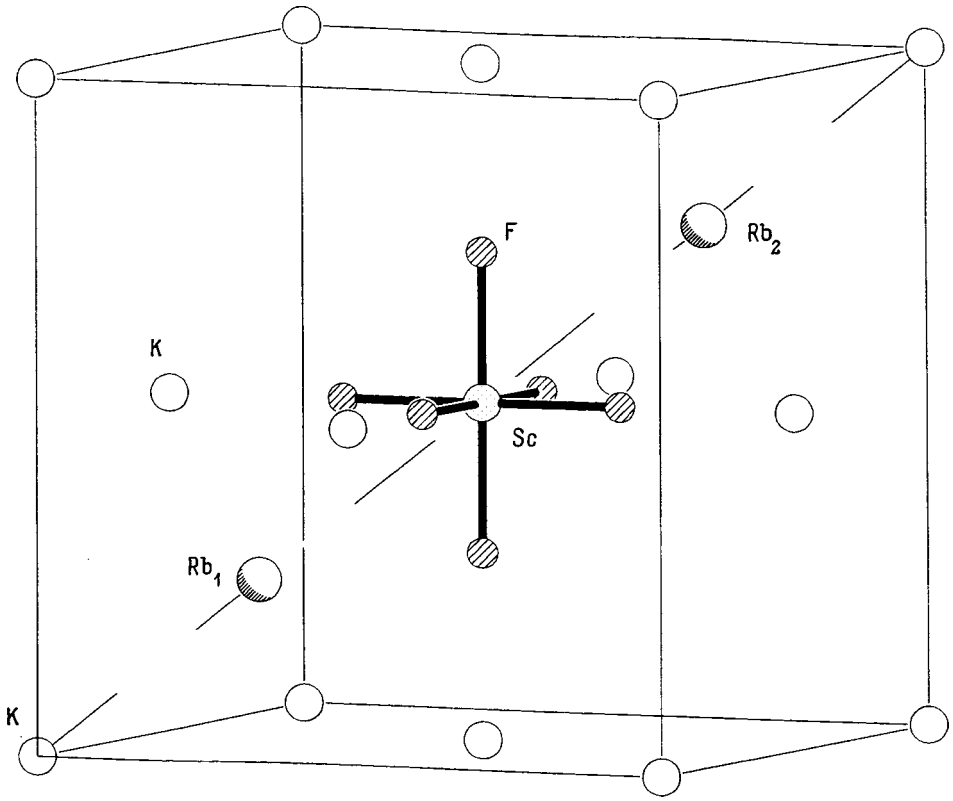

FIG. 1. Crystal structure of Rb_2KScF_6 in the cubic phase. One molecule and the face-centered K lattice are shown.

Rb_2KScF_6 crystals in unstable cubic and tetragonal phases and in the stable monoclinic phase, on the basis of the generalized Gordon–Kim model proposed by Ivanov and Maksimov.[3]

The model and computational method for calculating the frequencies of the normal lattice vibrations and the high-frequency permittivity are presented in Sec. 1. The computational results and their discussion are presented in Sec. 2.

1. MODEL. COMPUTATIONAL METHOD

The model proposed by Ivanov and Maksimov[3] for an ionic crystal, taking account of the polarizability of the ions, is used to calculate the phoon frequency spectrum of Rb_2KScF_6. In this model the ionic crystal is modeled by individual, overlapping, spherically symmetric ions. The total electron density of the crystal is written as

$$\rho(\mathbf{r})=\sum_i \rho_i(\mathbf{r}-\mathbf{R}_i),$$

where the summation extends over all ions in the crystal.

The total energy of the crystal in the density functional method, taking account of only a pair interaction, has the form

$$E_{\rm cr}=\frac{1}{2}\sum_{i\neq j}\frac{Z_iZ_j}{|\mathbf{R}_i-\mathbf{R}_j|}+Z_iE_i^{\rm self}(R_w^i)+\frac{1}{2}\sum_{i\neq j}\Phi_{ij}(R_w^i,R_w^j,|\mathbf{R}_i-\mathbf{R}_j|), \quad (1)$$

where Z_i is the charge of the i-th ion,

$$\Phi_{ij}(R_w^i,R_w^j,|\mathbf{R}_i-\mathbf{R}_j|)=E\{\rho_i(\mathbf{r}-\mathbf{R}_i)+\rho_j(\mathbf{r}-\mathbf{R}_j)\}-E\{\rho(\mathbf{r}-\mathbf{R}_i)\}-E\{\rho(\mathbf{r}-\mathbf{R}_j)\}, \quad (2)$$

the energy $E\{\rho\}$ is calculated by the density functional method[4] using a local approximation for the kinetic and

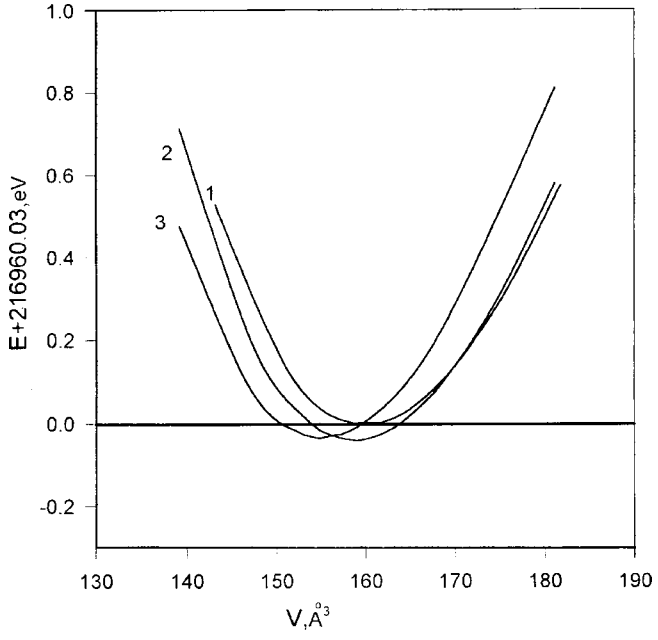

FIG. 2. Total energy (per molecule) of Rb_2KScF_6 versus the volume. Curve *1* — cubic phase, curve *2* — tetragonal phase, curve *3* — monoclinic phase.

TABLE I. The equilibrium values of the lattice parameters.

Phase	Space group	a, Å		b, Å		c, Å	
		Calculation	Experiment	Calculation	Experiment	Calculation	Experiment
Cubic	$Fm3m$	8.60	9.02	8.60	9.02	8.60	9.02
Tetragonal	$I4/m$	6.08	6.37	6.08	6.37	8.60	9.00
Monoclinic	$P12_1/n1$	6.03	6.36	6.03	6.36	8.52	8.99

Note. Experimental values from Ref. 2.

exchange-correlation energies, and $E_i^{\text{self}}(R_w^i)$ is the self-energy of an ion. The electronic energy and the self-energy of an individual ion are calculated taking account of the crystal potential approximated by a charged sphere (Watson sphere)

$$v(r)=\begin{cases} Z^{\text{ion}_i}/R_w & r<R_w, \\ Z_i^{\text{ion}}/r & r>R_w, \end{cases} \tag{3}$$

where R_w is the radius of the Watson sphere. The radii R_w^i of the spheres at individual ions are determined so as to minimize the total energy of the crystal.

To calculate the lattice dynamics, terms describing energy changes caused by displacements of the ions from their equilibrium positions must be added to the crystal energy (2). An expression for the dynamical matrix taking account of the electronic polarizability of the ions and the ''breathing'' of an ion in the crystal environment for crystals of arbitrary symmetry is given in Ref. 5. The results of a group-theoretic analysis of the phonon spectrum of crystals having the elpasolite structure are also presented there. We employ the results in Ref. 5 to calculate the vibrational frequencies of the Rb_2KScF_6 lattice and their symmetry classification.

The Coulomb contribution to the dynamical matrix was calculated by Ewald's method. The calculation of an ion was performed using Liberman's program,[6] and the pair interaction energy (3) and polarizability of an ion were calculated using the Ivanov–Maksimov program,[3] the Thomas–Fermi approximation for the kinetic energy, and the Hedin–Lundquist approximation for the exchange correlation energy. The technique of approximating the energy dependences on the distances **R** and the potentials v of the Watson sphere were used to calculate the derivatives appearing in the dynamical matrix. Chebyshev polynomials were used for the approximations.[3]

2. RESULTS AND DISCUSSION

In this section the computational results for the total energy, the equilibrium volume, and the phonon spectra of Rb_2KScF_6 in three phases are presented.

2.1. Cubic phase

The equilibrium lattice parameter was determined from the minimum in the volume dependence of the total energy of the crystal (Fig. 2). The lattice parameters together with the experimental values are presented in Table I. It is evident from Table I that the computed values of the lattice parameters (for cubic and tetragonal and monoclinic phases) agree to within 5% with the experimental data. The radii of the Watson spheres found for the ions Rb^+, K^+, and F^- by minimizing the total energy are 2.5, 2.5, and 2.625 a.u., respectively. The Sc^{3+} ion was calculated without a Watson sphere, since our calculations for the cubic phase show that the radii of the scandium ion in a Watson sphere and in the free state are virtually identical. Table II gives the computed polarizabilities of the ions, the high-frequency permittivity, and the dynamic ion charges in an Rb_2KScF_6 crystal.

The computed dispersion curves of the phonon frequencies of Rb_2KScF_6 in the cubic phase are shown in Fig. 3, and the limiting phonon frequencies ($\mathbf{q}=0$) are presented in Table III. Table III table also gives the experimental values

TABLE II. The polarizabilities of the ions, the high-frequency permittivity, and the dynamic charges.

Atom	Cubic $\varepsilon_\infty=1.91$				Tetragonal $\varepsilon_\infty^{xx}=1.92$, $\varepsilon_\infty^{zz}=1.95$				Monoclinic* $\varepsilon_\infty^{xx}=1.94$, $\varepsilon_\infty^{yy}=1.93$, $\varepsilon_\infty^{zz}=1.94$			
	α, Å^3	Z_{xx}	Z_{yy}	Z_{zz}	α, Å^3	Z_{xx}	Z_{yy}	Z_{zz}	α, Å^3	Z_{xx}	Z_{yy}	Z_{zz}
Rb	1.35	1.27	1.27	1.27	1.35	1.25	1.25	1.31	1.35	1.01	1.01	1.01
K	0.78	1.21	1.21	1.21	0.78	1.20	1.20	1.21	0.78	1.02	1.02	1.02
Sc	0.29	3.30	3.30	3.30	0.29	3.25	3.25	3.32	0.29	3.0	3.0	3.0
F_1	0.79	−0.97	−0.97	−1.58	0.81	−0.96	−0.96	−1.60	0.81	−0.93	−0.93	−1.16
										−0.94	−0.94	−1.03
F_2	0.79	−0.97	−1.58	−0.97	0.81	−1.33	−1.18	−0.99	0.81	−1.08	−1.02	−0.93
										−1.02	−1.08	−0.93
F_3	0.79	−1.58	−0.97	−0.97	0.81	−1.18	−1.33	−0.99	0.79	−1.02	−1.08	−0.98
										−1.08	−1.02	−0.98

*In the monoclinic phase the dynamic charges of the fluorine ions belonging to different octahedra in the unit cell are different; this is reflected in the table.

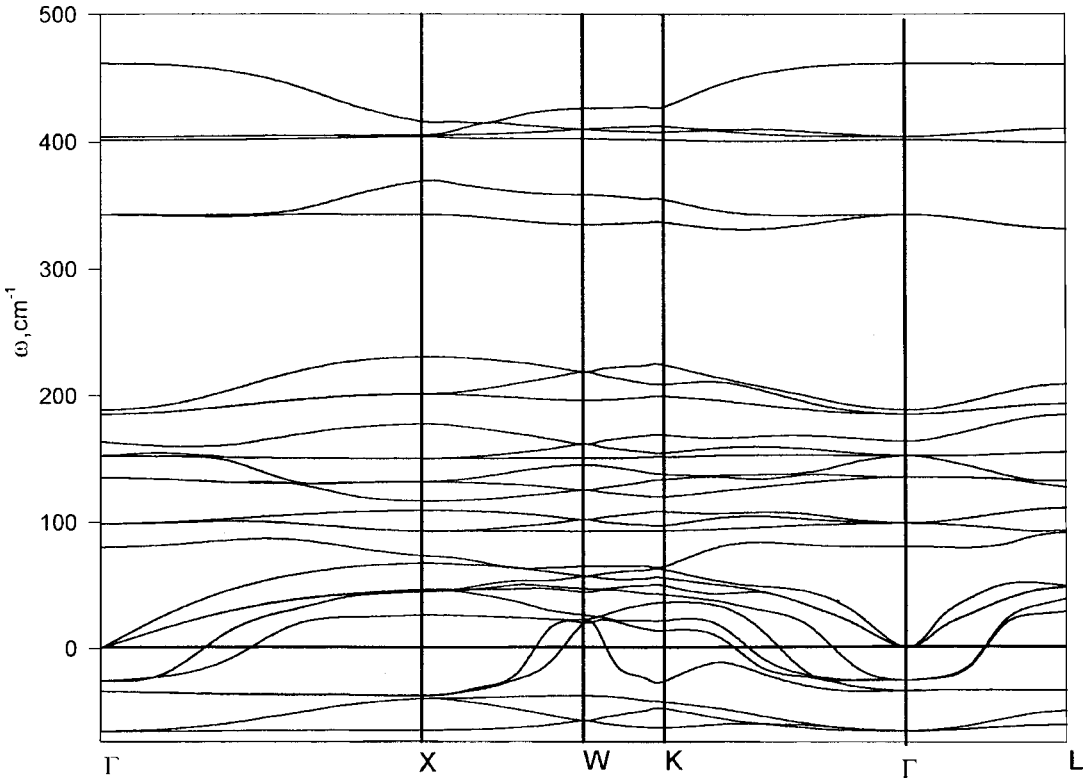

FIG. 3. Computed dispersion curves of Rb_2KScF_6 in the cubic phase. The imaginary frequencies are shown as negative values.

of some Raman-active vibrational frequencies measured in Ref. 7. One can see that the computed values of the Raman-active limiting frequencies are 10–20% less than the experimental values.

As one can see from Fig. 3 and Table III, there exist imaginary phonon frequencies. This attests to structural instability of the cubic phase in this material. It should be underscored that the unstable modes occupy the entire phase

TABLE III. Limiting vibrational frequencies ($\mathbf{q}=0$) in the cubic and tetragonal phases.

	Cubic				Tetragonal		
ω_i, cm^{-1}	Degeneracy	Vibration type	Frequency	Experiment[7]	Degeneracy	Vibration type	Frequency
ω_1	3	T_{1g}	66.2i		2	E_g	53.6i
					1	A_g	20.1
ω_{2T}	2	T_{1u}	34.3i		1	A_u	14.6i
					1	E_u	14.5
ω_3	3	T_{2g}	26.0i	80.0	1	B_g	18.4
					2	E_g	22.7
ω_4	3	T_{1u}	0.0		1	A_u	0.0
					2	E_u	0.0
ω_{2L}	1	T_{1u}	80.2		1	E_u	82.0
ω_5	3	T_{2u}	98.9		2	E_u	102.9
					1	B_u	111.9
ω_{6T}	2	T_{1u}	135.3		1	A_u	132.7
					1	E_u	136.9
ω_7	3	T_{2g}	152.4	230.0	2	E_g	151.5
					1	B_g	151.7
ω_{6L}	1	T_{1u}	163.7		1	E_u	160.3
ω_{8T}	2	T_{1u}	185.2		1	A_u	180.0
					1	E_u	183.6
ω_{8L}	1	T_{1u}	188.6		1	E_u	187.5
ω_9	2	E_g	342.9	400.0	1	A_g	325.1
					1	B_g	335.7
ω_{11}	1	A_{1g}	401.6	510.0	1	A_g	384.5
ω_{10T}	2	T_{1u}	404.1		1	A_u	390.4
					1	E_u	406.3
ω_{10L}	1	T_{1u}	461.5		1	E_u	443.0

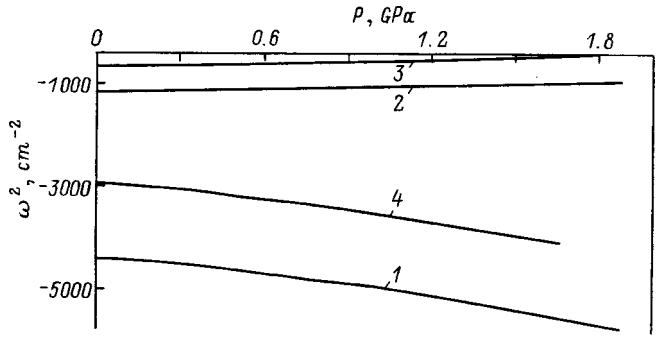

FIG. 4. $\omega_i^2(\mathbf{q})$ versus the pressure. Cubic phase: Curve *1* — $\omega^2_{T_{1g}}$ ($\mathbf{q}=0$); curve *2* — $\omega^2_{T_{1u}}$ ($\mathbf{q}=0$); curve *3* — $\omega^2_{T_{2g}}$ ($\mathbf{q}=0$); tetragonal phase: *4* — $\omega^2_{X_3}$ ($\mathbf{q}=1/2(\mathbf{b}_1+\mathbf{b}_2)$).

space in the Brillouin zone and the absolute values of these unstable modes are comparable in magnitude at the symmetric points of the Brillouin zone. The experimentally observed phase transitions in the Rb_2KScF_6 crystal are associated with the instability of the modes at the center and at the boundary point X of the Brillouin zone. In what follows we shall discuss the vibrational modes belonging to these points.

Three types of instability of the cubic structure occur at the center of the Brillouin zone. The greatest instability (the largest, in absolute magnitude, negative value of the squared frequency of the normal mode) is associated with the triply degenerate mode T_{1g}, in which only four fluorine atoms are displaced from positions of equilibrium[5,8]

$$-F_{1y}=F_{2y}=F_{5z}=-F_{6z},$$

$$-F_{1x}=F_{2x}=-F_{3z}=F_{4z},$$

$$-F_{3y}=F_{4y}=-F_{5x}=F_{6x}.$$

These displacements lead to rotation of the ScF_6 octahedra as a whole. The second type of instability, a ferroelectric instability, is associated with transverse vibrations of the polar mode T_{1u}. In this mode all atoms in a unit cell are displaced from positions of equilibrium of the cubic phase. As far as we know, ferroelectric phase transitions in halide crystals with elpasolite structure have not been observed experimentally. Finally, instability of the third type is associated with the triply degenerate mode T_{2g}. In one of the characteristic vectors of this mode, the atomic displacements cause the ScF_6 octahedra to rotate around the body diagonal with a simultaneous displacement of the rubidium atoms located on this diagonal toward one another. It should be noted that

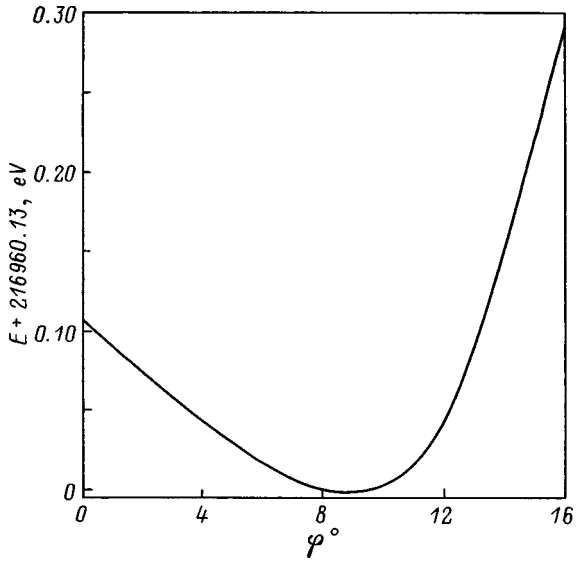

FIG. 5. Total energy of Rb_2KScF_6 versus the rotation angle of ScF_6 octahedra in the tetragonal phase.

there is also a stable mode with the same symmetry T_{2g} in the phonon spectrum of an Rb_2KScF_6 crystal (see Table III).

The strongest lattice instability at the points X on the Brillouin boundary is related with the nondegenerate X_3 mode, in which the displacements of the four fluorine ions ($F_{3y}=-F_{4y}=F_{5z}=-F_{6z}$) also correspond to rotation of ScF_6 octahedra as a whole, but this rotation is not uniform throughout the crystal and the condensation of this mode results in doubling of the unit-cell volume.

As we have already mentioned in the introduction, as the temperature decreases, a transition to the tetragonal phase associated with condensation of the ''soft'' T_{1g} mode at the center of the Brillouin zone occurs first in the Rb_2KScF_6 crystal. Under hydrostatic pressure the temperature of this phase transition shifts in the direction of high temperatures, with $dT_{c1}/dP=16.6$ K/GPa.[9] We can estimate the derivative dT_{c1}/dP from our calculations assuming that the phase-transition temperature is proportional to the absolute value of the squared frequency of the soft mode T_{1g}. The pressure was determined by differentiating numerically the volume dependence of the total energy. The hydrostatic pressure dependence of the frequencies of the soft modes at the center of the Brillouin zone is shown in Fig. 4. It is evident that the lattice softens under pressure with respect to the T_{1g} mode and hardens with respect to all other unstable modes. The derivative dT_{c1}/dP was found to be $\sim$40 K/GPa, which

TABLE IV. Computed and experimental[2] coordinates of atoms in the tetragonal phase $I4/m$.

Atom	Position		Filling		x/a,	x/a,	y/b,	y/b,	z/c,	z/c,
	theory	experiment	theory	experiment	theory	experiment	theory	experiment	theory	experiment
Rb	4*d*	4*d*	1	1	0.5	0.5	0.0	0.0	0.25	0.25
K	2*b*	2*b*	1	1	0.0	0.0	0.0	0.0	0.25	0.25
Sc	2*a*	2*a*	1	1	0.0	0.0	0.0	0.0	0.0	0.0
F_1	4*e*	16*i*	1	1/4	0.0	0.05	0.0	0.01	0.22	0.22
F_2	8*h*	16*i*	1	1/2	0.19	0.20	0.25	0.24	0.0	−0.03

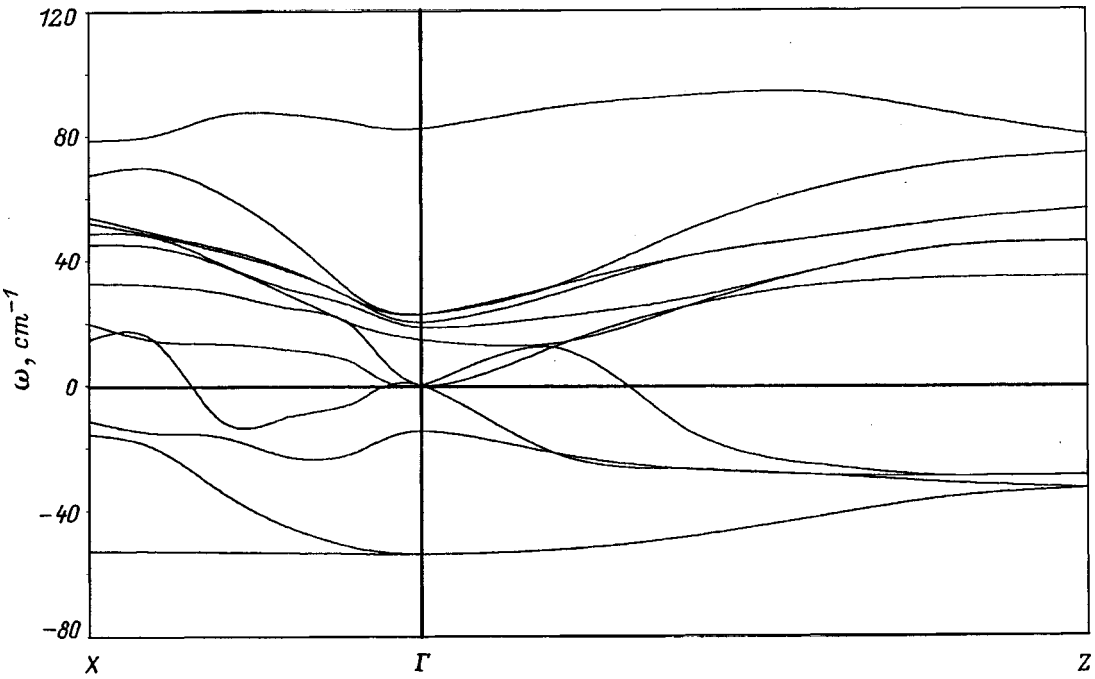

FIG. 6. Low-frequency part of the computed dispersion spectrum in two symmetric directions in the Brillouin zone of Rb_2KScF_6 in the tetragonal phase. The imaginary frequencies are shown as negative values.

is more than two times larger than the experimental value.

2.2. Tetragonal phase

The phase transition to the tetragonal phase is related to condensation of one component of the triply degenerate T_{1g} mode at the center of the Brillouin zone. This condensation corresponds to rotation of ScF_6 octahedra around a principal axis of the cubic phase. The space group of the tetragonal phase is $I4/m$ and the unit cell contains one molecule. The distortion of the cubic phase (the rotation angle of an octahedron) was determined from the minimum of the total energy as a function of rotation angle, which is shown in Fig. 5. In calculating this dependence, for each fixed value of the rotation of an octahedron, the total energy was minimized with respect to the cell parameters and with respect to the radii of the Watson spheres of the ions. It is evident from Fig. 5 that the minimum of the total energy corresponds to the rotation angle $\varphi = 8°$. However, the calculation is performed at $T = 0$, while the tetragonal phase exists at a finite temperature in a quite narrow temperature range (~ 30 K). The phase transition $Fm3m \rightarrow I4/m$ is of second order[1] and the order parameter in the temperature interval $T/T_{c1} = 0.9$ is far from saturation (for example, in the mean-field approximation it is 0.6), so that distortions corresponding to the rotation angle of an octahedron $\varphi = 5°$ were used to calculate the energy and frequency spectrum in the tetragonal phase. The volume dependence of the total energy in the tetragonal phase is shown in Fig. 2. The equilibrium values obtained for the unit-cell parameters and coordinates of the atoms are presented together with the experimental data in Tables I and IV, whence one can see that the computed values of the cell parameters are approximately 4% lower than the experimental values. At the same time the computed displacements of the fluorine ions from positions of equilibrium in the cubic phase are larger than the experimental data by approximately the same amount.

The computed values of the permittivity and dynamic Born charges of an Rb_2KScF_6 crystal in the tetragonal phase are presented in Table I. One can see that a tetragonal distortion leads to a redistribution of the dynamic charges on the fluorine ions. We calculated the phonon frequency spectrum of an Rb_2KScF_6 crystal in the tetragonal phase for all symmetry directions and points of the Brillouin zone. However, to save space we do not present here all of the results of these calculations, since the spectrum of ''nonsoft'' modes changes negligibly compared with the spectrum of these modes in the cubic phase (naturally, the lowering of the symmetry lifts the degeneracy of the modes). For this reason, the computed values of the limiting phonon frequencies are presented in Table II and the lower part of the frequency spectrum for two symmetric directions of the Brillouin zone is shown in Fig. 6. As one can see from Table II and Fig. 6, a structural instability ouccrs in the tetragonal phase of Rb_2KScF_6 just as in the cubic phase, but the number of ''soft'' modes in this phasebecomes less than in the cubic phase. It should be underscored that the number of unstable vibrational modes in the tetragonal phase depends strongly on the rotation angle of the ScF_6 octahedra. Figure 7 shows the dependence of the frequencies of several ''soft'' modes at the center and boundary point X of the Brillouin zone versus the rotation angle of the octahedra. It is evident from this dependence that, as the rotation angle of the octahedra increases, the absolute magnitude of the squared frequencies of the ''soft'' modes decreases and for $\varphi \sim 12°$ the squared frequencies become positive (for all modes in the Brillouin

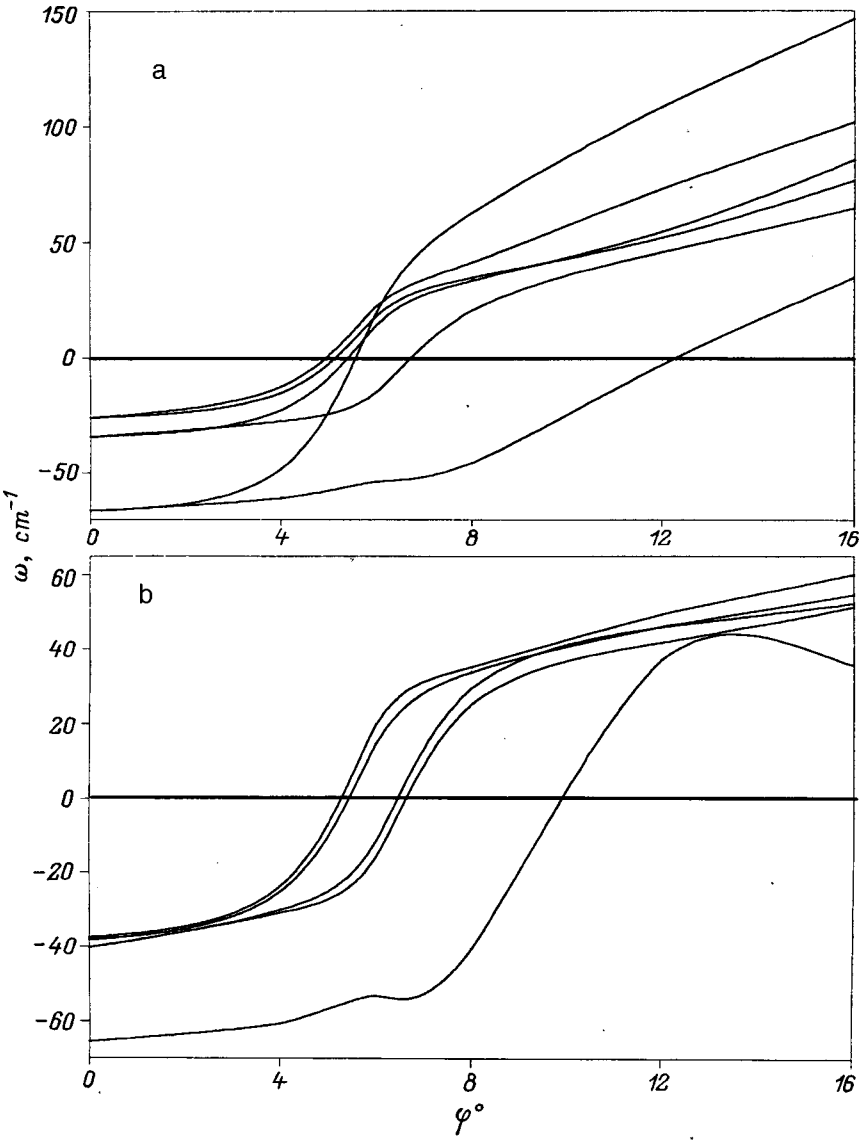

FIG. 7. ''Soft'' lattice vibrational frequencies versus the rotation angle of ScF_6 octahedra in the tetragonal phase: a — Center of the Brillouin zone $\mathbf{q}=0$; b — boundary point X of the Brillouin zone $\mathbf{q}=1/2(\mathbf{b}_1+\mathbf{b}_2)$. The imaginary frequencies are shown as negative values.

zone), i.e. the tetragonal phase is stable for such displacements of the fluorine ions.

As we have already mentioned above, the tetragonal phase in the Rb_2KScF_6 crystal exists at temperatures between 250 and 220 K. At $T_{c2}=220$ K a second phase transition occurs in this crystal into the monoclinic phase, whose unit cell is doubled compared with the cells of the cubic and tetragonal phases. As follows from the results of structural investigations of the monoclinic phase of Rb_2KScF_6,[2] the cell doubling is due to the condensation of the unstable mode at the boundary point X of the Brillouin zone of the tetragonal group $I4/m$.

As one can see from Fig. 6, the computed frequencies of the unstable modes at the center and at the point X of the Brillouin zone are comparable in absolute magnitude, and

TABLE V. Computed and experimental[2] coordinates of atoms in the monoclinic phase $P12_1/n1$.

Atom	Position	Filling	x/a, theory	x/a, experiment	y/b, theory	y/b, experiment	z/c, theory	z/c experiment
Rb	4*e*	1	0.500	0.504	0.00	−0.02	0.254	0.251
K	2*c*	1	0.0	0.0	0.0	0.0	0.5	0.5
Sc	2*a*	1	0.0	0.0	0.0	0.0	0.0	0.0
F_1	4*e*	1	0.030	0.058	−0.030	0.011	0.220	0.221
F_2	4*e*	1	−0.250	−0.252	0.190	0.189	0.023	0.029
F_3	4*e*	1	0.190	0.184	0.250	0.256	0.000	−0.031

TABLE VI. Limiting vibrational frequencies ($\mathbf{q}=0$) in the monoclinic phase.

ω_i, cm^{-1}	Frequency	ω_i, cm^{-1}	Frequency	ω_i, cm^{-1}	Frequency	ω_i, cm^{-1}	Frequency
1	0.0	16	74.9	31	142.6	46	226.1
2	0.0	17	78.5	32	145.1	47	230.7
3	0.0	18	82.1	33	153.8	48	273
4	21.0	19	87.5	34	161.2	49	316.3
5	26.6	20	90.6	35	163.3	50	317.3
6	33.4	21	93.2	36	173.9	51	319.8
7	41.3	22	102.2	37	181.7	52	353.0
8	41.8	23	108.8	38	197.0	53	391.7
9	42.0	24	114.6	39	199.2	54	398.1
10	46.6	25	118.5	40	206.3	55	400.0
11	49.4	26	122.8	41	206.7	56	402.2
12	54.3	27	127.9	42	209.7	57	403.5
13	55.4	28	131.1	43	216.7	58	406.2
14	66.5	29	131.7	44	221.6	59	439.6
15	68.8	30	134.7	45	224.2	60	461.5

the unstable modes, just as in the cubic phase, occupy a large volume of the phase space. Analysis of the characteristic vectors of the unstable modes shows that vibrational modes in which the displacements of atoms correspond to a ''pure'' rotation of ScF_6 octahedra do not exist in the tetragonal phase. At the boundary point X of the Brillouin four fluorine and rubidium ions are displaced in the most unstable mode:

$$F_{1x}=-F_{2x}\approx F_{1y}=-F_{2y},$$

$$F_{5z}\approx -0.75F_{6z},$$

$$\mathrm{Rb}_{1z}=\mathrm{Rb}_{2z},$$

and these displacements produce a monoclinic distortion of the tetragonal phase with cell doubling.

It has been established experimentally[9] that under hydrostatic pressure the temperature of the phase transition from the tetragonal to the monoclinic phase shifts in the direction of high temperatures. The computed hydrostatic pressure dependence of the squared frequency of the most unstable mode at the boundary point X is shown in Fig. 4, whence it is evident that this dependence agrees qualitatively with the experimental dependence. However, the numerical estimate $dT_{c2}/dP\sim 60$ K/GPa differs strongly from the experimental value of 3.2 K/GPa.[9]

2.3. Monoclinic phase

The coordinates of the atoms in the monoclinic phase, calculated according to the displacements corresponding to condensation of the mode X_3 of the tetragonal phase, are presented in Table V. The table also gives the experimental values of these coordinates. It is evident that the displace-

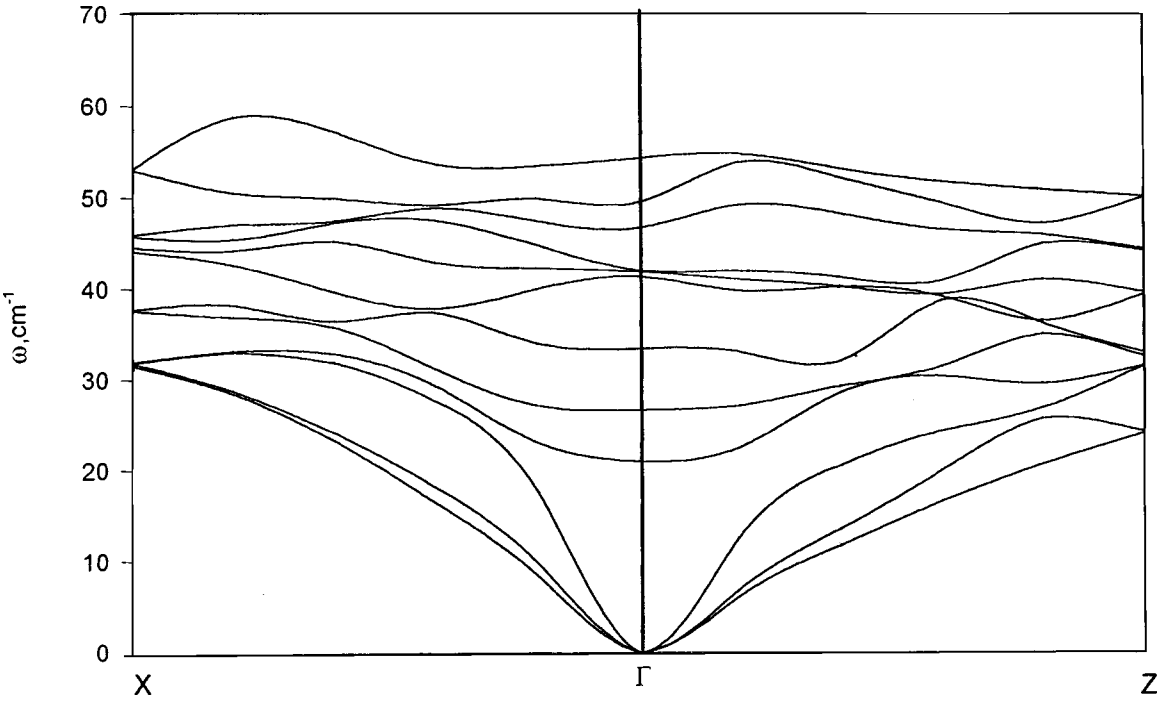

FIG. 8. Low-frequency part of the computed dispersion curve in two symmetric directions in the Brillouin zone of Rb_2KScF_6 in the monoclinic phase.

ments of the ions F_1 and F_3 in the experimentally determined structure differ substantially from the displacements of these ions as a result of condensation of mode X_3. The computed total energy of Rb_2KScF_6 in the monoclinic phase, for the computed coordinates of the atoms, was found to be 0.14 eV higher than the values of the total energy calculated from the coordinates of the experimental structure. The volume dependence of the energy using the experimental values of the coordinates is presented in Fig. 3, and the values of the unit-cell parameters together with the experimental values are presented in Table I. There are no unstable vibrational modes in the computed phonon frequency spectrum of the monoclinic phase of Rb_2KScF_6. The limiting phonon frequencies are presented in Table VI, and Fig. 8 shows the dispersion curve of the low-frequency part of the spectrum for two symmetric directions in the Brillouin zone of the monoclinic group $P2_1/n1$.

In summary, the static and dynamic properties of a Rb_2KScF_6 crystal with elpasolite structure in the cubic, tetragonal, and monoclinic phases were calculated in the present work on the basis of a fairly simple nonempirical model of an ionic crystal. The computed equilibrium values of the lattice parameters are in satisfactory agreement with the experimental data. At the same time the computed Raman phonon frequencies are 10–20% less than the experimental values. This discrepancy could be due to the fact that, in the present approach, the calculations of the lattice dynamics neglected the higher, specifically the quadrupole, distortions of the electron density, which for the present class of compounds are different from zero even in a static lattice because the fluorine ions are located in a noncubic environment.

The results obtained on the instability of cubic and tetragonal structures, the stability of the monoclinic phase in a Rb_2KScF_6 crystal, and the effect of hydrostatic pressure on the phase transition temperatures describe the experimental situation qualitatively correctly.

We thank O. V. Ivanov and E. G. Maksimov for the opportunity to use their computational program to calculate the total energy and polarizability of ions.

We thank the Russian Fund for Fundamental Research (Grant No. 97-02-16277) and INTAS (Grant No. 10-177) for financial support.

*)E-mail: zinenko@iph.krasnoyrsk.su

[1] I. N. Flerov, M. V. Gorev, K. S. Aleksandrov, A. Tressaud, J. Grannec, and M. Couzi, Mater. Sci. Eng. R. **24**, 81 (1998).
[2] H. Faget, J. Grannec, A. Tressaud, V. Rogriguez, T. Roissnel, I. N. Flerov, and M. V. Gorev, Eur. J. Solid State Inorg. Chem. **33**, 893 (1996).
[3] O. V. Ivanov and E. G. Maksimov, Zh. Eksp. Teor. Fiz. **108**, 1841 (1995) [JETP **81**, 1008 (1995)].
[4] W. Kohn and L. J. Sham, Phys. Rev. A **140**, 1113 (1965).
[5] V. I. Zinenko, N. G. Zamkova, and S. N. Sofronova, Zh. Eksp. Teor. Fiz. **114**, 1742 (1998) [JETP **87**, 944 (1998)].
[6] D. A. Liberman, D. T. Cromer, and J. J. Waber, Comput. Phys. Commun. **2**, 107 (1971).
[7] H. Guengard, Doctoral Thesis, Université de Bordeaux (1994).
[8] M. Couzi, S. Khairoun, and A. Tressaud, Phys. Status Solidi A **98**, 423 (1986).
[9] I. N. Flerov, M. V. Gorev, S. V. Mel'nikova, S. V. Misyul', V. N. Voronov, and K. S. Aleksandrov, Fiz. Tverd. Tela (Leningrad) **34**, 2185 (1992) [Sov. Phys. Solid State **34**, 1168 (1992)].

Translated by M. E. Alferieff